Nucleic Acids Research, 2024, **52**, 4111–4123
https://doi.org/10.1093/nar/gkae199
Advance access publication date: 30 March 2024
Critical Reviews and Perspectives

Critical steps in the assembly process of the bacterial 50S ribosomal subunit

Amal Seffouh[1,2], Rainer Nikolay[3] and Joaquin Ortega[1,2,*]

[1]Department of Anatomy and Cell Biology, McGill University, Montreal, Quebec H3A 0C7, Canada
[2]Centre for Structural Biology, McGill University, Montreal, Quebec H3G 0B1, Canada
[3]Department of Genome Regulation, Max Planck Institute for Molecular Genetics, 14195 Berlin, Germany
[*]To whom correspondence should be addressed. Tel: +1 905 577 3750; Email: joaquin.ortega@mcgill.ca

Abstract

During assembly, ribosomal particles in bacteria fold according to energy landscapes comprised of multiple parallel pathways. Cryo-electron microscopy studies have identified a critical maturation step that occurs during the late assembly stages of the 50S subunit in *Bacillus subtilis*. This step acts as a point of convergency for all the parallel assembly pathways of the subunit, where an assembly intermediate accumulates in a 'locked' state, causing maturation to pause. Assembly factors then act on this critical step to 'unlock' the last maturation steps involving the functional sites. Without these factors, the 50S subunit fails to complete its assembly, causing cells to die due to a lack of functional ribosomes to synthesize proteins. In this review, we analyze these findings in *B. subtilis* and examine other cryo-EM studies that have visualized assembly intermediates in different bacterial species, to determine if convergency points in the ribosome assembly process are a common theme among bacteria. There are still gaps in our knowledge, as these methodologies have not yet been applied to diverse species. However, identifying and characterizing these convergency points can reveal how different bacterial species implement unique mechanisms to regulate critical steps in the ribosome assembly process.

Graphical abstract

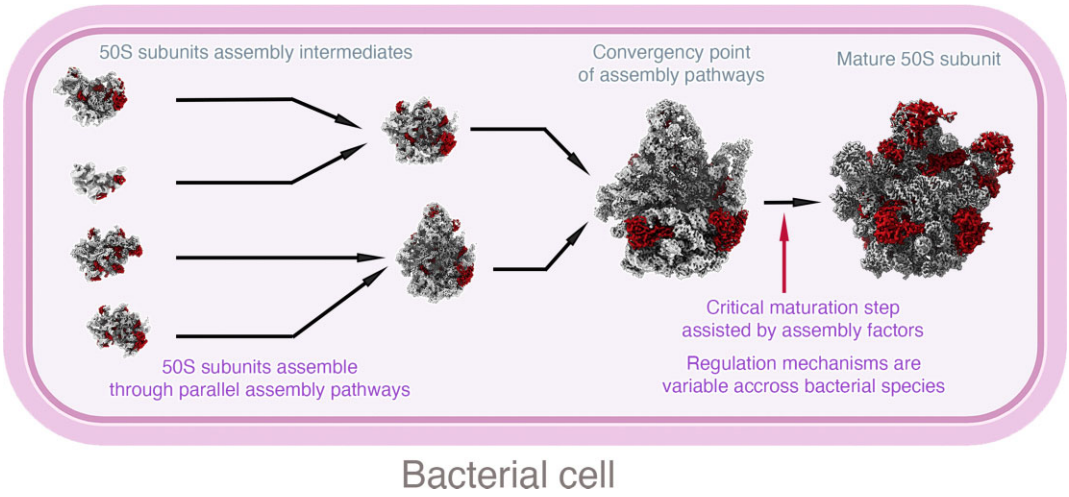

Introduction: maturation of the bacterial 50S subunit in the context of the ribosome assembly process

Ribosomes in bacteria are formed rapidly and accurately to support cellular growth demands and ensure proper translation of the genetic code. Recently, significant advances in our understanding of the bacterial ribosome assembly process have been made possible through the use of cryo-electron microscopy (cryo-EM). This technology has allowed for near-atomic resolution structures and a better mechanistic understanding of highly heterogeneous specimens. Cryo-EM structures of ribosomal particles captured at various stages of assembly provide increasingly detailed models of the assembly process and a precise description of how multiple trans-acting proteins, called assembly factors, mediate critical steps of the process.

The bacterial 70S ribosome comprises two subunits: the small (30S) and large (50S) subunits. It consists of more than fifty distinct ribosomal proteins (r-proteins) and three ribosomal RNAs (rRNA) that have to fold and associate in a

Received: September 14, 2023. **Revised:** March 2, 2024. **Editorial Decision:** March 6, 2024. **Accepted:** March 7, 2024

time-coordinated manner. The process of assembling the ribosome starts with transcribing a single rRNA precursor transcript containing the three rRNA molecules for the two subunits. The 30S subunit contains 16S rRNA, while the 50S subunit contains 23S and 5S rRNAs. Initially, RNAase III splits the three rRNA fragments, and then additional RNAases remove the remaining nucleotides in both their 5′ and 3′ ends (precursor sequences), resulting in mature 16S, 23S and 5S rRNA molecules (1).

The 30S and 50S subunits assemble independently before associating as a functional 70S ribosome. The folding of the rRNA components for each subunit starts immediately after transcription commences and even before the rRNA is completely processed. The initial folds adopted by the rRNA motifs are rapidly bound hierarchically by r-proteins (2,3), stabilizing these local RNA structures and inducing subsequent conformational changes that create new binding sites for other r-proteins to enter the assembling particle (4,5). The r-proteins typically assist early folding stages of the rRNA molecules (6–9). However, additional proteins called 'assembly factors' are also required to catalyze the folding of the rRNA at the late stages of assembly (10). As the rRNA folds or once the folding is completed, another group of enzymes introduces modifications, mainly involving methylation (11) and pseudouridylation (12) of nucleotides located in the ribosome functional sites, the decoding center in the 30S subunit and peptidyl transferase center (PTC) in the large subunit. Importantly, when considered separately, none of the individual rRNA modifications are essential for cell survival despite their high degree of conservation among bacterial species.

In the assembly of the 50S subunit, which is the focus of this review, the 23S and 5S rRNA molecules are thought to fold according to a funnel-shaped energy landscape similar to those driving protein folding (Figure 1). This energy landscape reflects the multiple parallel pathways that outline a process with built-in redundancy, ensuring efficient ribosome assembly even under non-favourable conditions (13,14). Initially, it was postulated that the 50S assembly is a parallel process from beginning to end, and all assembly pathways converge in the mature 50S subunit. However, recent work in *Bacillus subtilis* has revealed that, at least in this species, the parallel assembly pathways converge into a critical maturation step (15–17). This step represents a merging point where all parallel assembly pathways of the ribosomal particles converge (Figure 1). The assembly intermediate accumulating at the convergency point exists in a 'locked' state, and its maturation is paused. Unlocking this intermediate and completing its maturation requires the coordinated action of multiple assembly factors. These factors license further maturation steps to convert this particle into a mature 50S subunit. In *B. subtilis*, factors acting at the convergency points are essential, and in their absence, cells die due to a lack of functional ribosomes to synthesize proteins.

Whereas the existence of 'locked' convergency points in the 50S assembly pathway of *B. subtilis* has been established, it is still unclear whether they also exist in other bacterial species. Below, we will review the various methodologies recently employed to capture 50S assembly intermediates and enable their structural characterization. These methods vary depending on how closely they mimic the cellular environment where ribosome biogenesis occurs. These approaches involved studies in *B. subtilis* and *E. coli*, the model organisms for Gram-positive and Gram-negative bacteria. Gaps do still exist, as each methodology has yet to be applied to these two model organisms and other organisms evolutionary distant from *B. subtilis* and *E. coli*. Here, we will review the available structures observed with these methods to summarize what is presently known on the existence of 'locked' convergency points in the 50S assembly pathway of *B. subtilis* and *E. coli*. We will also analyze how different species use distinctive sets of assembly factors to regulate the locking mechanism and eventually license the last maturation steps, which enable the 50S subunit to associate with the 30S subunit and initiate protein synthesis.

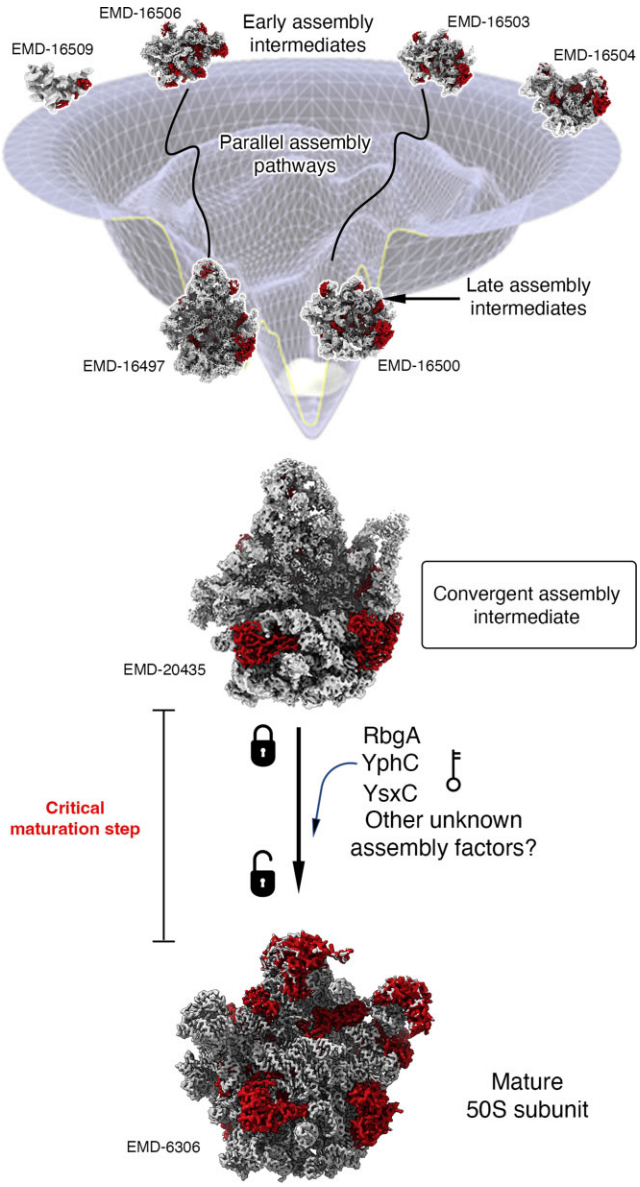

Figure 1. Overview of the 50S subunit assembly process in *B. subtilis*. The 50S ribosomal particles at the early stages of assembly follow parallel assembly pathways that converge into a critical maturation stage. The assembly intermediate that accumulates is 'locked', and its maturation is paused. RbgA, YphC and YsxC act on this intermediate to 'unlock' it and complete the maturation of the ribosomal particle. The rRNA in the cryo-EM maps is colored in light gray, and the r-proteins are shown in red. This figure was prepared from EMD entries 16 497, 16 500, 16 509, 16 506, 16 503, 16 504 (30), 20 435 (17) and 6306 (56).

Methodologies used to structurally characterize the maturation process of the 50S subunit and what they provide

Actively growing bacteria are highly efficient in assembling ribosomal subunits (18,19). Consequently, an intrinsic challenge in studying the ribosome assembly process is the transient nature of assembly intermediates, making them short-lived and difficult to capture in sufficient amounts. In the last decade, various groups have used several approaches to trigger the accumulation of assembly intermediates. Conceptually, the various methods differ in how much each relies upon the environment of a living cell to generate the ribosome assembly intermediates. Using these methods, researchers find a trade-off between the detailed studies achievable through *in vitro* experiments focused solely on assembly (20), and the less precise but more biologically relevant studies carried out in living cells (21).

The genetic approach is the most commonly used method within purely *in vivo* studies that generate ribosome intermediates in living cells. This approach has been instrumental in dissecting the function of specific assembly factors that mainly assist the late stages of assembly. The approach relies on the creation of single knockouts (for non-essential genes) (22,23) or deletion strains (for essential genes) (15,16,24) for genes encoding specific assembly factors, causing bacteria to slow down their ribosome assembly process significantly. Under these conditions, cells accumulate a complex heterogeneous mixture of ribosome assembly intermediates that are informative on the maturation reaction catalyzed by the assembly factor. These studies have shown that some of the intermediates in the mixture can be bound by the removed assembly factor when provided *in trans*, indicating they represent their actual substrates (25,26). Importantly, these studies also showed that the immature particles that accumulate can evolve into functional mature subunits, and they are not dead-end assembly products (15,27).

Fully *in vitro* studies in ribosomal assembly are also possible because of the remarkable property of both ribosomal subunits to assemble in the complete absence of any additional cellular factors except from its purified rRNA and r-protein components (2,3). These reconstitution experiments leverage Nomura´s paradigm that the blueprint of ribosome assembly is inherent to the participating rRNA and protein molecules. However, ribosome *in vitro* reconstitution assays require extended incubation times, high salt concentrations and elevated temperatures to overcome those energy barriers typically catalyzed by ribosome assembly factors. In the case of the 50S subunit, the reconstitution reaction has two main steps (20,28,29) (Figure 4A). In the first step of the reaction, the r-proteins, 23S and 5S rRNA molecules are mixed and incubated at 44°C for 30 min. At the end of this incubation, 41S and 48S intermediates are formed. In the second step, the magnesium concentration is adjusted to 20 mM and the mixture is incubated at 50°C for 90 min. During this step, the 41S and 48S particles convert into the mature state and become functional in protein translation. In vitro reconstitution assays are valuable because they provide a minimum system for studying the assembly pathways intrinsic to the ribosome components.

Assembly factors *in vivo* provide speed and directionality to the assembly process by catalyzing the formation and maturation of assembly intermediates along a few selected pathways from the myriad of possibilities in the folding landscape. These so-called 'canonical' pathways are the most efficient routes to ensure that assembly is efficient and that the number of particles becoming trapped in dead-end assembly intermediates is minimized. *In vitro* ribosome reconstitution assays allow us to explore the assembly pathways that the ribosomal particles can follow without assembly factors to reach the mature state. In a first approach, 50S *in vitro* reconstitution assays combined with cryo-EM analyses yielded high resolution structures of 50S assembly intermediates at the medium and late stages of their assembly (20). However, more recently, limiting the incubation time in the *in vitro* reconstitution reaction to just 3 minutes enabled the capture of structural snapshots of pre-50S intermediates at very early stages of their assembly. These intermediates comprise as few as 500 nucleotides of rRNA and 3 r-proteins in a folded conformation (30).

Finally, the method merging the advantages of ribosome assembly *in vivo* approaches with the flexibility of the *in vitro* systems is the integrated rRNA synthesis, ribosome assembly, and translation reaction (iSAT). This method was initially described in 2013 (31) and is an *in vitro* system since the reaction occurs outside a cellular environment. However, unlike the *in vitro* ribosome reconstitution assays described above, the primary rRNA transcript is transcribed during the incubation period in the presence of processing enzymes, r-proteins and assembly factors provided *in trans*. Under the iSAT reaction conditions, the assembly of the particles occurs co-transcriptionally, mirroring the process in the cell. Nevertheless, the efficiency of the assembly in the iSAT reaction is lower than that observed *in vivo*, most likely because the transcription rate, r-protein and assembly factor concentration are more tightly regulated inside the cell than under the conditions of the iSAT reaction. In contrast to the classical reconstitution protocols, the iSAT reaction does not require drastic changes in the incubation temperature, and the reaction is typically maintained at 37°C (31–34) and 10 mM Mg^{2+}. Even though the concentration of free Mg^{2+} in the bacterial cytoplasm is lower than 10 mM Mg^{2+} (∼1–2 mM) (35), the incubation conditions of the iSAT reaction are more similar to the cytoplasmic environment in bacterial cells. Importantly, the reaction incorporates the translation of a reporter, such as GTP or luciferase, to monitor the production of active ribosomes. The iSAT reaction has recently been shown to be an extremely powerful tool to generate 50S assembly intermediates at early, intermediate, and late assembly stages that have been characterized by cryo-EM (36).

The 50S assembly pathways of *Bacillus subtilis* contain convergency points before reaching the mature state

Cryo-EM analyses of 50S assembly intermediates purified from *B. subtilis* RbgA, YphC and YsxC depletion strains (16) have revealed that the late stages of maturation in the large subunit involve the folding of the central protuberance, the L1 and L7/12 stalks and the functional core (A, P and E sites) (Figure 2A). The 50S assembly intermediates that accumulate upon depletion of these three GTPases are called $45S_{RbgA}$, $45S_{YphC}$ and $44.5S_{YsxC}$ and show that these regions are still immature. The r-proteins uL16, bL27, bL28, bL33, bL35 and bL36, which are located at the base of the central protuberance have not been incorporated into any of the three assembly intermediates (Figure 2B, C) (15,16). An important finding was that the $45S_{RbgA}$, $45S_{YphC}$ and $44.5S_{YsxC}$

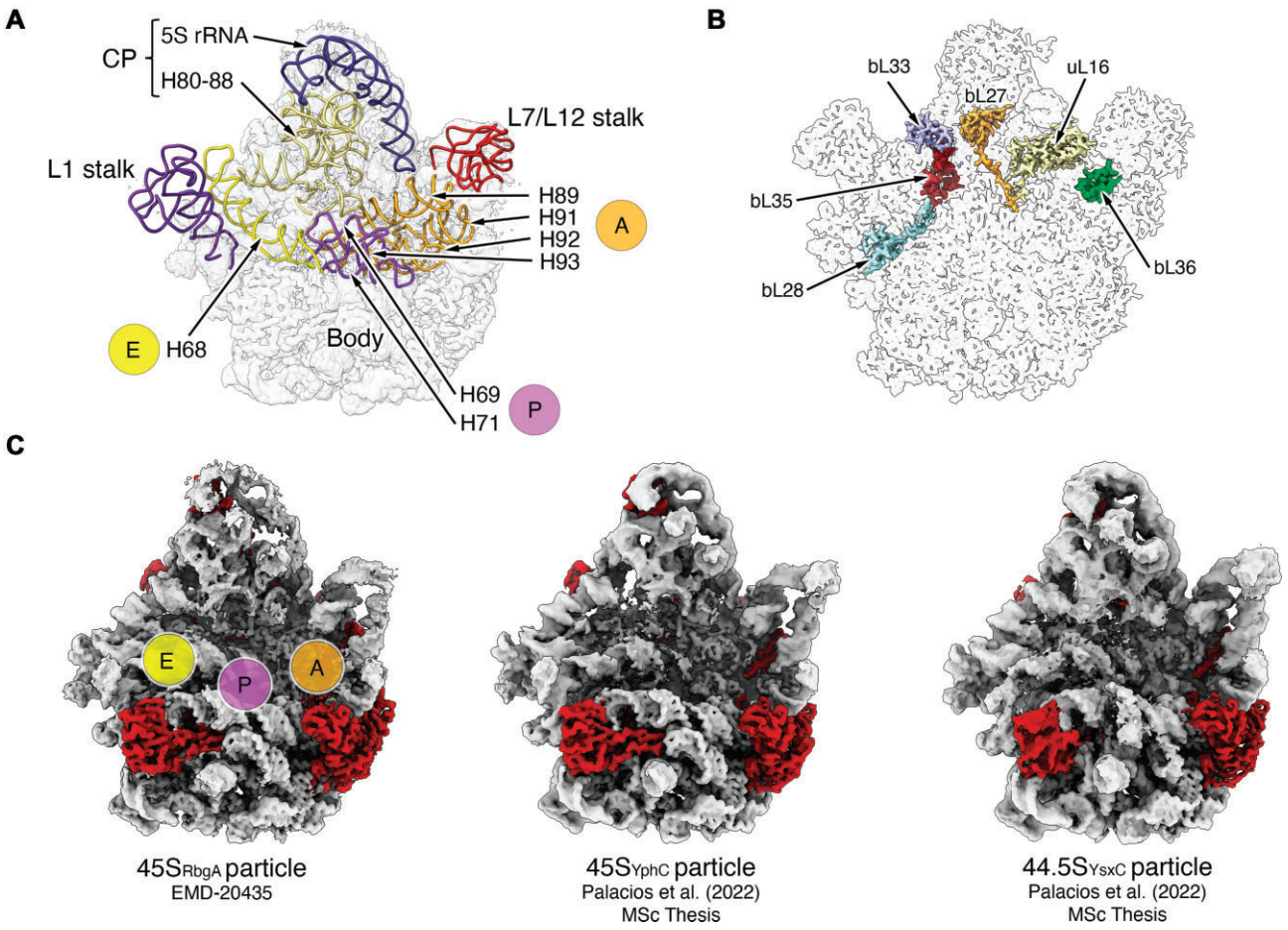

Figure 2. Convergency points in the 50S assembly pathway of *B. subtilis*. (**A**) The late stages of assembly in the 50S subunit involve the maturation of the central protuberance (CP), the L1 and L7/12 stalks and the functional core (A, P and E sites). Panel A shows these landmarks overlaid in the structure of the mature 50S subunit. The rRNA helices comprising the A, P and E site are indicated. The components of the central protuberance, 5S rRNA and H80-88 are also indicated. (**B**) The assembly intermediates that accumulate under depletion of assembly factors RbgA (45S$_{RbgA}$), YphC (45S$_{YphC}$) and YsxC (44.5S$_{YsxC}$) present depletion of r-proteins uL16, bL27, bL28, b33, b35 and b36. The panel shows the location of these proteins in the mature 50S subunit structure. Panels (A) and (B) were produced from PDB 3J9W (56). (**C**) Cryo-EM structures of the 45S$_{RbgA}$, 45S$_{YphC}$ and 44.5S$_{YsxC}$ particles showing that these assembly intermediates are structurally similar. The rRNA in the cryo-EM maps is colored in light gray, and the r-proteins are shown in red. Structure representations were prepared from EMD entries 20435 (25) (45S$_{RbgA}$) and (57) (45S$_{YphC}$ and 44.5S$_{YsxC}$).

assembly intermediates are identical in the r-proteins they contain (16) and remarkably similar in structure (Figure 2C). They are also 'promiscuous', and every particle can bind individually to each of the GTPases. These results suggested that particles assemble through the multiple parallel pathways comprised in the folding landscape of the rRNA. However, regardless of the individual maturation pathway taken by each individual particle, they all end up evolving into a convergent assembly intermediate (Figure 1). RbgA, YphC and YsxC are essential (37,38) for this convergent assembly intermediate to mature further and become a functional 50S subunit. In the absence of any of the three factors, the 50S subunit does not complete its assembly, and cells die due to a lack of functional ribosomes to synthesize proteins.

Among these three essential factors, the role of RbgA is the best understood. Upon binding to the 45S$_{RbgA}$ particle, RbgA induces rRNA helices forming the P-site (the functional site housing the tRNA that holds the growing polypeptide chain of amino acids during protein synthesis), and the A site (binding site for the charged tRNA molecules during protein synthesis) to adopt their mature conformation. RbgA binding also has an overall stabilizing effect in the r-protein uL6 and the rRNA helices forming the L1 stalk, H38 and central protuberance (25) (Figure 3A). Importantly, GTP binding is required for RbgA to recognize the 45S$_{RbgA}$ particles. However, energy from GTP hydrolysis is unnecessary for triggering any conformational changes that evolve the particle towards the mature state.

One significant aspect of the maturation reaction catalyzed by RbgA is that most of the maturation steps performed by assembly factors can still occur spontaneously but with less efficiency. However, the presence of RbgA is essential to the maturation process of 45S$_{RbgA}$ particles. A genetic study from the Britton's lab suggesting a functional interaction between RbgA and ribosomal protein uL6 (39), provided the first hint on the essentiality of RbgA. This study showed that a strain expressing the RbgA-F6A variant generates spontaneous single-point mutations within the N-terminal domain of uL6. Each suppressor strain accumulated a novel 44S ribosomal particle that matured into 50S subunits. The cryo-EM structures of the 44S particles from two uL6 suppressor strains, 44S$_{R3C}$ and 44S$_{R70P}$ revealed that these 44S particles are identical to the 45S$_{RbgA}$ particles, except that the incorporation of uL6 R3C and uL6 R70P variants in the 44S particles

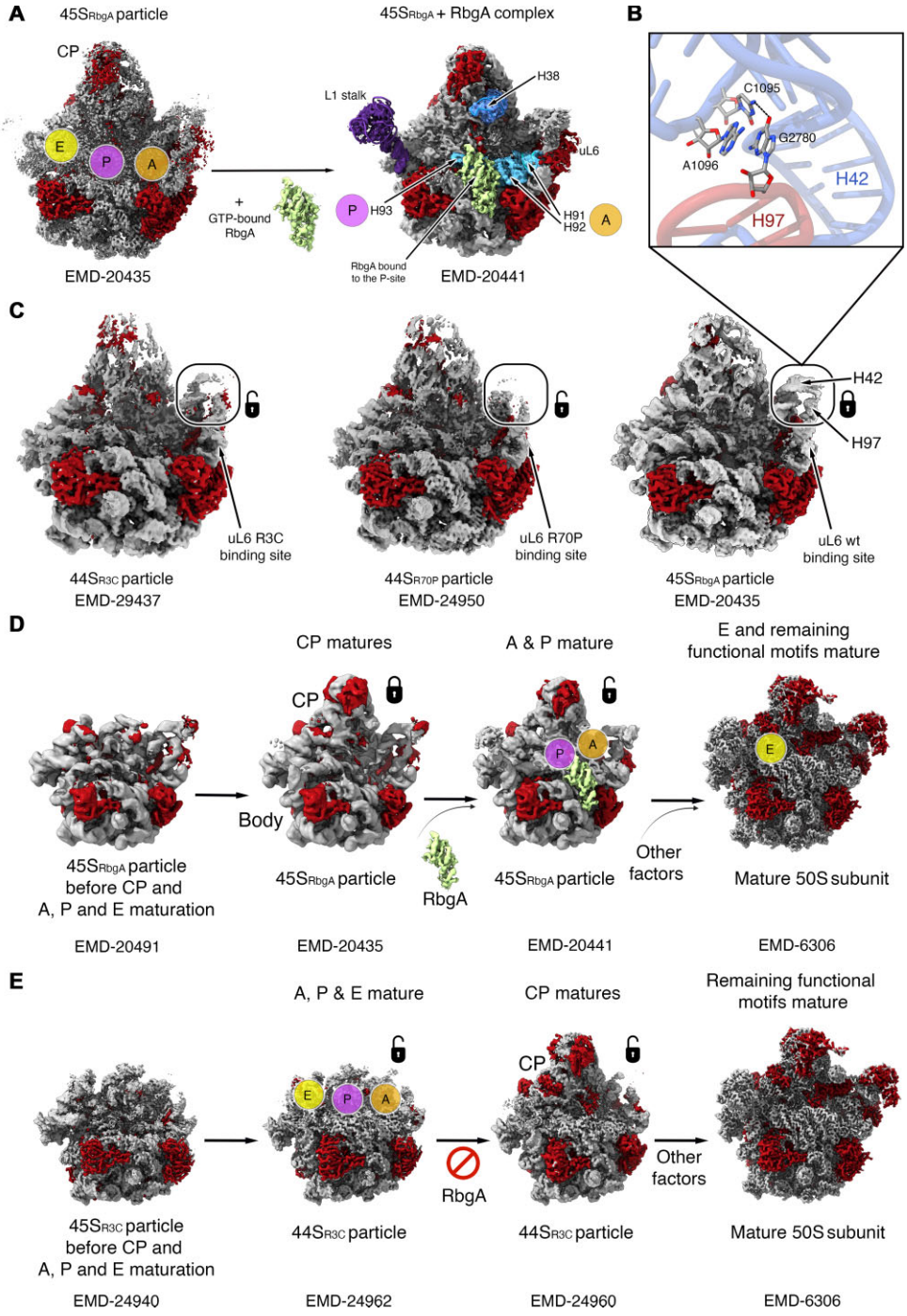

Figure 3. The essential role of RbgA at the critical maturation steps of the 50S subunit in *B. subtilis*. (**A**) This panel shows how RbgA binding to the P site in the 45S$_{RbgA}$ assembly intermediate triggers the folding of critical rRNA helices in the A site (H91 and H92) and P site (H93), all colored in cyan. RbgA binding also stabilizes the L1 stalk (colored in dark blue), H38 (colored in purple) and the binding of r-protein uL6. The remaining rRNA helices are shown in light gray and all r-proteins are shown in red. Structure representations were prepared from EMD entries 20 435 and 20 441 (25). (**B**) The rRNA helices H97 and H42 in the 45S$_{RbgA}$ particle are latched together through the atomic interactions shown in the panel, locking the maturation of the intermediate and making it dependent on RbgA to continue its maturation process. (**C**) This panel shows how H97 and H42 are linked in the cryo-EM structure of the 45S$_{RbgA}$ particle. The binding of r-protein uL6 stabilizes this interaction. The lack of uL6 incorporation in the case of the R70P uL6 variant or the incorporation of the uL6 R3C variant into the corresponding 44S particles causes H97 and H42 to remain unlatched, making the 44S intermediates less dependent on RbgA to continue their maturation. Structure representations were prepared from EMD entries 29 437 (44S$_{R3C}$), 24 950 (44S$_{R70P}$) (17) and 20 435 (45S$_{RbgA}$) (25). (**D**) The panel shows the canonical maturation pathway of the 45S$_{RbgA}$ particle where maturation of the functional A, P and E sites occurs after the central protuberance (CP). Binding of uL6 and the dependency of RbgA for this maturation steps ensure this specific order for the maturation of this critical structural motifs of the 50S subunit. Structure representations were prepared from EMD entries 20 491, 20 435 and 20 441 (25) and 6306 (56). (**E**) In the 44S$_{R3C}$ particles, incorporating the R3C uL6 variant allows maturation to evolve through an alternative pathway. In this case, the maturation of these intermediates is less dependent on RbgA and the maturation of the functional sites is possible before the central protuberance develops. The 44S$_{R70P}$ particle matures following a similar pathway but it is not shown in the panel. Structure representations were prepared from EMD entries 24 940, 24 960, 24 962 (17) and 6306 (56). In panels (C)–(E), the rRNA in the cryo-EM maps is colored in light gray, and the r-proteins are shown in red.

prevented the stabilization of helices H97 and H42 near the binding site of uL6 (Figure 3C). These two helices are latched together in the $45S_{RbgA}$ particles containing wild-type uL6, forming a stable structural motif that pauses maturation (Figure 3B, C). The $45S_{RbgA}$ particles require RbgA binding to continue their maturation process and follow a precisely defined maturation pathway that ensures that the A, P and E functional sites always mature after the central protuberance (Figure 3D). In contrast, we found the $44S_{R3C}$ and $44S_{R70P}$ particles, where the helices H97 and H42 are not latched together, pursue alternative maturation pathways in which assembly of the functional sites occurs ahead of the central protuberance (Figure 3E). Furthermore, the $44S_{R70P}$ particles mature spontaneously in a completely RbgA-independent manner.

These studies revealed that RbgA is essential for the $45S_{RbgA}$ particles to continue their maturation process because it 'unlocks' the conformation imposed by uL6 binding. RbgA is like the 'key' that opens the H97–H42 'lock' imposed by uL6 binding. Binding of RbgA licenses further folding of the functional core of the subunit, but only in particles with a fully assembled central protuberance. By this mechanism, RbgA ensures that the maturation of the functional sites occurs last and only after the central protuberance has been formed (Figure 3D). In doing so, RbgA ensures ribosomal particles only engage in translation when their maturation is completed. This is important for cell survival, as immature ribosomes generate toxic proteins caused by translation errors (40). An additional role of RbgA is to keep the assembling particles in the maturation pathway with the highest efficiency and with a lower frequency of generating dead-end intermediates that fail to complete maturation.

Regarding YphC and YsxC, the other two essential factors for the late stages of maturation of the 50S subunit to be completed, their exact role is still uncharacterized. However, these two factors likely assist the folding of the other rRNA helices in which RbgA does not participate. The three factors may also assist in the recruitment and stabilization of the r-proteins that are still missing from the $45S_{RbgA}$, $45S_{YphC}$ and $44.5S_{YsxC}$ particles (Figure 2B, C). How they participate in the unlocking mechanism of the 45S particle is still unknown.

Are convergency points in the 50S subunit assembly process common among bacterial species?

RbgA, YphC and YsxC are widely distributed in the genomes of Gram-positive and Gram-negative bacteria genomes, including important human pathogens such as *Vibrio cholerae* and *Neisseria meningiditis* (37). However, RbgA, YphC and YsxC factors are absent in important model bacteria (i.e. RbgA is absent in *E. coli*), and even when these factors are present in a bacterial genome, they are not always essential genes like in *B. subtilis*. Consequently, it is still unknown whether the convergence point observed in the 50S assembly process in *B. subtilis* also exists in other bacterial species. If so, how is the locking mechanism implemented for species lacking RbgA, YphC or YsxC proteins?

In *E. coli*, researchers have used *in vitro* reconstitution reactions of the 50S subunit from purified components (20,30), the iSAT reaction (36) and the genetic approaches (41–44) to visualize assembly intermediates using cryo-EM. Below, we describe some of the intermediates structurally characterized in these studies and compare them to the 45S particles in *B. subtilis* to analyze whether convergency points do exist in the 50S assembly process of *E. coli*, the model organism for Gram-negative bacteria.

Time course cryo-EM analysis of the *in vitro* 50S reconstitution reaction from purified components (Figure 4A) was performed without any assembly factors (30). The study identified a total of 16 distinct precursors of the 50S subunit, including the earliest intermediate described so far (Figure 4B). This particle consisted of only the first ~500 nucleotides of 23S rRNA domain I and three ribosomal proteins (uL22, uL24 and uL29). This intermediate is referred to as *d1*. The authors introduced a new nomenclature, where the early assembly states are named according to the 23S rRNA domains whose cryo-EM densities they exhibit (i.e. *d1, d12, d16*, etc). Using this new naming system, states with similar folded rRNA domains but with additional r-proteins were named by extending their name with the additional elements (i.e. *d1_L4/L23*). Domains I, II, III and VI of the 23S rRNA along with their interacting r-proteins constitute the core of the 50S subunit. Late intermediates with these 23S rRNA domains folded are referred to as state C (for core) particles. Subsequent maturation states, characterized by the emergence of additional prominent domains like the central protuberance (CP) or helix 68 (H68), are denoted as C-CP or C-CP-H68 (Figure 4A, B). Previous ribosome assembly studies named individual states simply by ascending numbers (state 1, 2, etc.) (20) or subsequent combinations of letters and numbers (state B1, B2, C1, etc.) (36,41,44), which impedes comparability among studies.

In addition to proposing this new nomenclature, Qin *et al.* (30) found that the *d1* intermediate evolves into the C state using two parallel routes, *d126 or d136*. State C subsequently matures the central protuberance (CP), becoming the *C-CP* intermediate. Then the L1 stalk develops, reaching the C-CP-L28/L2 state, and finally, the functional helices in the A, P and E sites start evolving a defined density. This intermediate is termed *C-CP-H68*, which still requires additional folding of the rRNA helices in the functional core before it becomes a mature 50S subunit (Figure 4B, C).

Contrary to the assembly pathways observed in the *B. subtilis* 50S subunit using the RbgA depletion strain (Figure 3D) (25), it was found that in the *in vitro* reconstitution reaction of the 50S subunit in *E. coli*, incorporation of the 5S rRNA and folding of the 23S rRNA domain V (H80-88) to form the central protuberance was possible in the absence of a fully assembled core (30). Intermediates *d12-CP* and *d126-CP* are two examples of particle intermediates following this assembly pathway (Figure 4B). However, these types of intermediates, which develop a central protuberance without a complete core domain, were not present among the assembly intermediates purified from the *B. subtilis* RbgA depletion strain (Figure 3D) (25) or in the iSAT experiments with *E. coli* components (Figure 5A) (36). The fact that the iSAT study also described early and mid-assembly intermediates, but these types of intermediates were not observed suggests that the assembly pathway favoring the establishment of the central protuberance before the core is not preferred in an *in vitro* reaction in the presence of assembly factors. Nevertheless, a state comparable to *d126-CP* was observed in studies using *E. coli* cells lacking the DEAD-box helicase DeaD or ribosomal protein bL17 (44), indicating that it may also exist in an *in vivo* scenario.

We also noticed a unique aspect in the 50S maturation process in the iSAT reaction (36) and this is the chronology of maturation of the A, P and E site functional sites. In the in

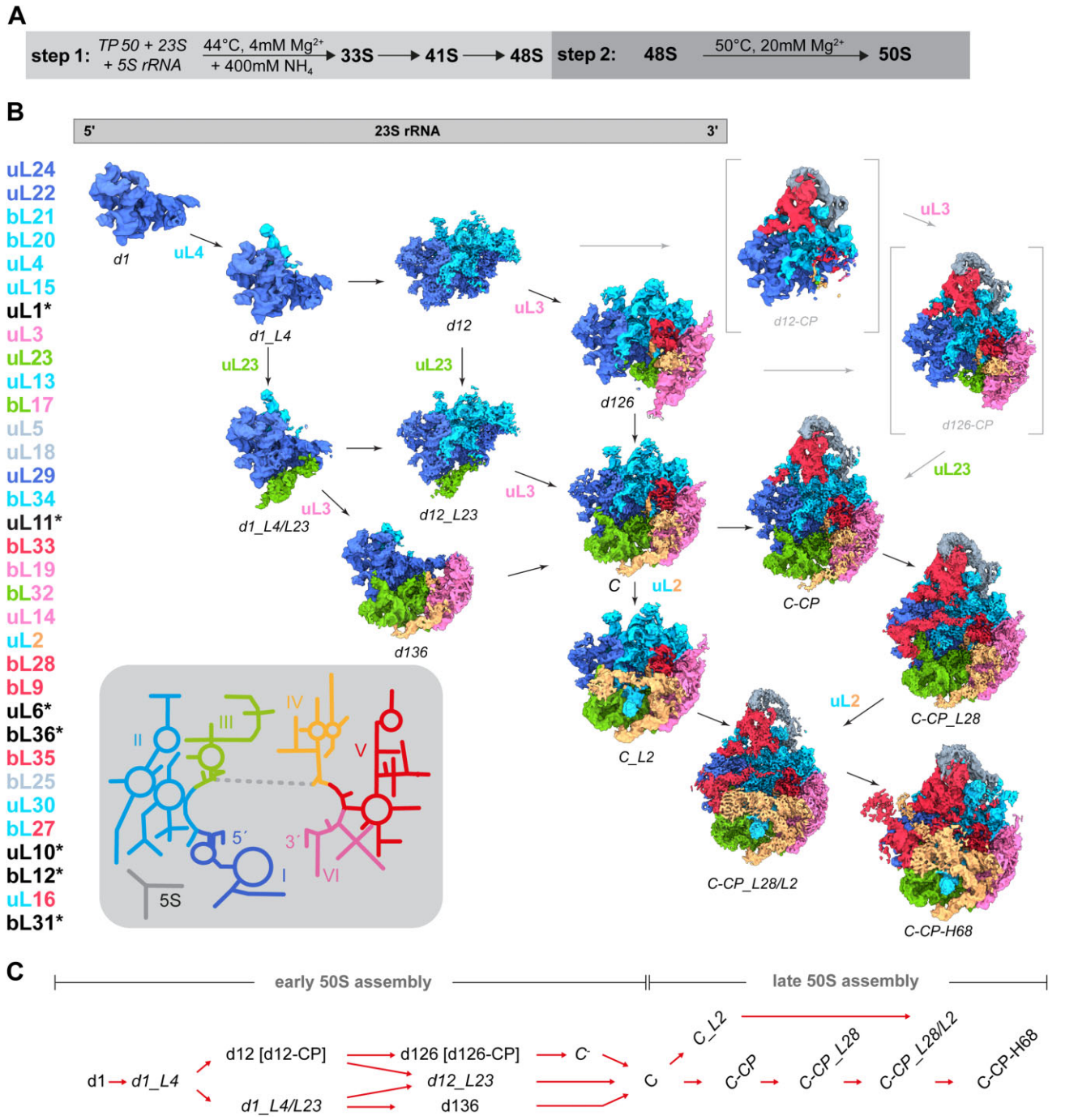

Figure 4. Assembly intermediates from an *in vitro* 50S reconstitution reaction from purified *E. coli* components. (**A**) Schematic of the 50S *in vitro* assembly assay, consisting of two steps. Under conditions indicated 33S, 41S and 48S precursors form during step 1. In step 2, the 48S precursor is converted into an active 50S subunit under the influence of heat (55°C) and 20 mM Mg^{2+}. (**B**) 50S assembly map based on the Nierhaus map (58), refined by Williamson (59). In contrast to the classical assembly map showcasing the order in which proteins bind to the RNA and the protein´s interdependencies, this map orders the precursor states obtained by cryo-EM analysis from material subjected to step 1 of the 50S reconstitution protocol (30). From left to right 5´of the 23S rRNA to 3´; from top to bottom order in which proteins were found to bind to the LSU *in vivo* (time). Particle densities in the cryo-EM maps are colored according to the architectural domains of the 23S rRNA they belong to. A 23S rRNA 2D map shown as insert appears in the same color code. All ribosomal proteins on the y-axis appear in the same color code. Structure representations were prepared from EMD entries 16 509 (d1), 16 508 (d1_L4), 16 507 (d1_L4/L23), 16 506 (d12), 16 505 (d12_L23), 16 502 (d12-CP), 16 503 (d126), 16 501 (d126-CP), 16 504 (d136), 16 499 (C), 16 498 (C_L2), 16 497 (C-CP), 16 496 (C-CP_L28), 16 494 (C-CP-H68) and 16 495 (C-CP_L28/L2) (30). (**C**) Nomenclature of the precursors. Early intermediates in this reaction are named according to the 23S rRNA domains whose cryo-EM densities were exhibited. Later, these intermediates extend their names by adding the name of the additional structural elements which density appears, such as L28, L2 or H68. Late maturation stages containing all domains of the core of the LSU (I, II, III and VI) are called C particles. The formation of the core demarcates the end of early 50S assembly. From there, particles that exhibit the central protuberance, add CP to their names. Different routes lead from state C to state C-CP-H68 (48S), the end point of step1 of 50S *in vitro* assembly. * Proteins not resolved in the cryo-EM maps.

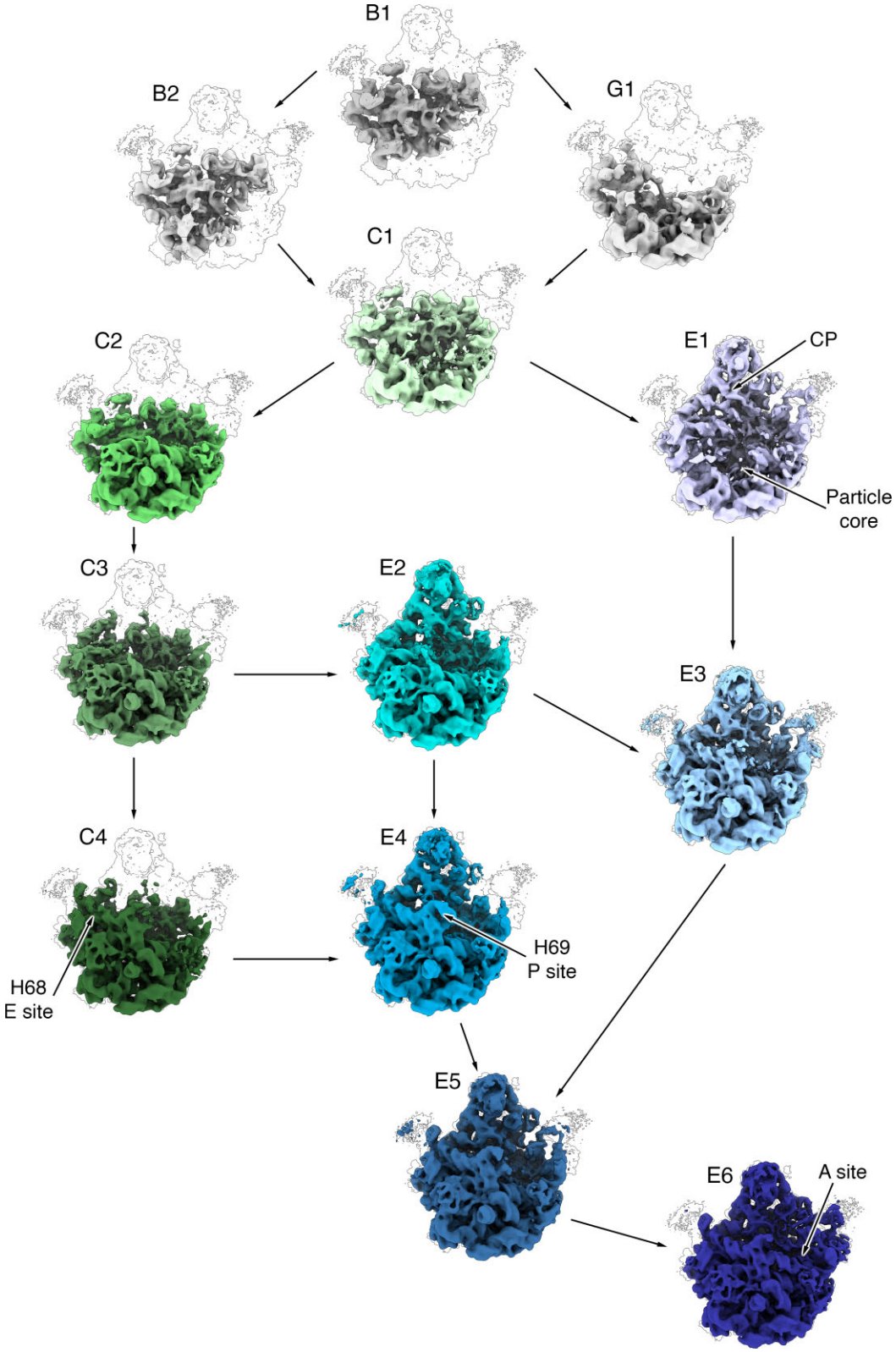

Figure 5. Assembly intermediates from an *in vitro* 50S reconstitution the iSAT reaction reaction from purified *E. coli* components. Cryo-EM maps obtained from the 50S assembly intermediates that accumulate in the iSAT reaction (36). Intermediates are named in this study using a subsequent combination of letters and numbers. The name of each intermediate is indicated in their upper left side. Key rRNA helices forming the P (H69) and E sites (H68) are indicated in intermediates where they become first apparent. The location of the A site, still partially immature is indicated in the most mature intermediate (E6). Structure representations were prepared from EMD entries 29 056 (B1), 29 042 (B2), 29 058 (C1), 29 059 (C2), 29 060 (C3), 29 061 (C4), 29 062 (E1), 29 063 (E2), 29 064 (E3), 29 065 (E4), 29 066 (E5), 29 067 (E6) and 29 057 (G1) (36).

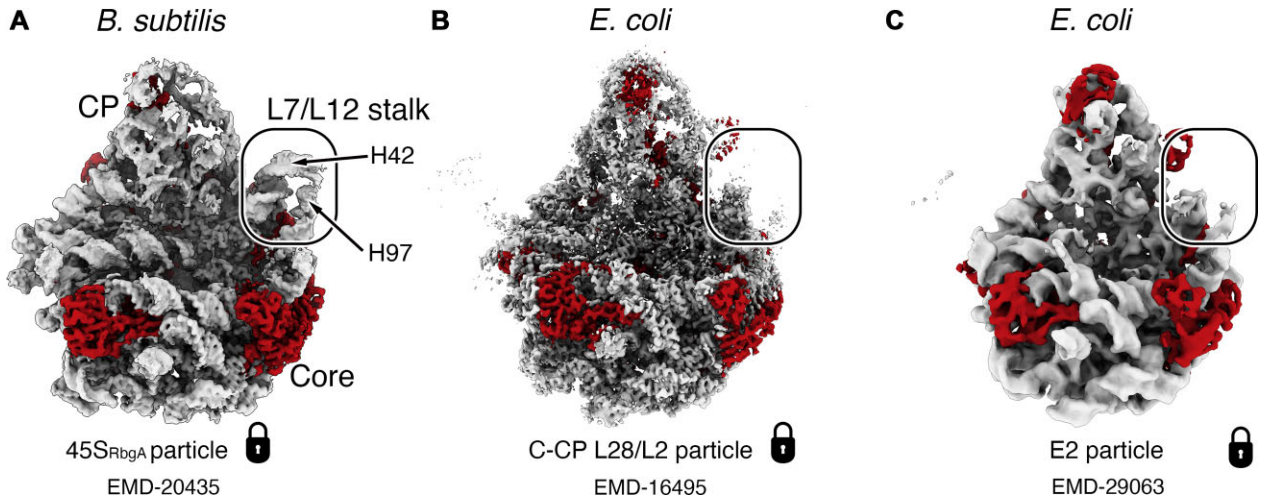

Figure 6. Convergency intermediates observed in *B. subtilis* and *E. coli* using various experimental methodologies. Structurally similar intermediates representing convergency points in the assembly process isolated using a RbgA-depletion *B. subtilis* strain (17,25) (**A**), an *in vitro* reconstitution assays with *E. coli* purified components (30) (**B**) and iSAT also with *E. coli* elements (36) (**C**). The name of the intermediate using the original terminology in each study is indicated below. The lock besides the name indicates that these three intermediates may represent a locked convergency point, requiring the interaction with assembly factors to progress into the mature 50S subunit. The assembly factors regulating the locked assembly point are still unknown in *E. coli* likely different from those described for RbgA in *B. subtilis*. In the three panels, the rRNA in the cryo-EM maps is colored in light gray, and the r-proteins are shown in red. This figure was prepared from EMD entries 20 435 (25) (45S$_{RbgA}$), 16 495 (C-CP-L28-L2) (30) and 29 063 (E2) (36).

vitro reconstitution assays with *E. coli* components (Figure 4A) (20,30), and the *in vivo* studies with the RbgA, YphC and YsxC depletion strains (Figure 3C), the three sites of the functional core in the 50S subunit always assemble last and after the central protuberance has been assembled (15,17,25,45). Intriguingly, in the iSAT reaction, a class with the core region formed but without central protuberance, named C4 particle, exhibited partially mature P and E sites with the long H68 already formed. Three additional classes also showed partially mature P and E sites while in the process of having the central protuberance still assembling (classes E3, E4 and E5) (Figure 5). Consequently, under iSAT experimental conditions it is only the A site, but not the P and E sites, the one functional site that is left to mature before any other structural motif.

Structurally, the E2 state in the iSAT reaction (36) and the *C-CP_L28/L2* state from the 50S *in vitro* reconstitution study (30) are the closest to the 45S intermediates isolated from the RbgA, YphC and YsxC depletion strains in *B.* subtilis, except for the L7/L12 stalk, where helices 97 and H42 near the binding site of uL6 are not latched together (Figure 6). The *C-CP-L28/L2* particle, similar to the 45S particle in *B. subtilis* is inactive in translation unless subjected to high Mg^{2+} concentration (20 mM) and thermal energy (50 °C) (20,46). This treatment transforms them into mature 50S subunits suggesting that the *C-CP_L28/L2* and *C-CP-H68* intermediates may represent a locked convergency point, requiring the interaction with assembly factors to progress into the mature 50S subunit. The assembly factors regulating the locked assembly point are still unknown in *E. coli* and the locking mechanism they implement are likely different from those described for RbgA in *B. subtilis*.

Genetic perturbations have also been employed to study the assembly process of the 50S subunit in *E. coli*. In three separate studies, cells were depleted from the DeaD cold shock protein (44), SrmB helicase (42) or ribosomal protein bL17 (41,43). In all cases, the assembly intermediates that accumulated resembled those observed using the iSAT reaction, and they could be arranged following similar parallel assembly pathways, suggesting that the iSAT reaction closely recapitulates the 50S assembly process *in vivo*.

How is the locking mechanism implemented in convergency points during the assembly process of the 50S subunit in *E. coli*?

The 50S *in vitro* reconstitution experiments (30), iSAT studies (36), and genetic approaches described in the previous section were important in identifying the potential existence of convergency points in *E. coli*. However, a study from the Suzuki group (47,48) suggested that in *E. coli*, the locking and unlocking mechanisms of the convergency intermediate are regulated by methylation. They found that RlmE, an S-adenosylmethionine-dependent methyltransferase catalyzes the 2′-*O*-methylation of uridine at position 2552 (Um2552) in helix 92 of the 23S rRNA. Deleting the *rlmE* gene in *E. coli* results in slow growth and accumulation of 45S particles. This particle is a genuine intermediate that can evolve into the mature 50S subunit and become a functional 70S ribosome (47). The study showed that the actual Um2552 modification, not the binding of RlmE to the methylation site, is important for the 45S intermediate to progress to a mature subunit.

The structure of this 45S particle from *E. coli* was obtained by cryo-EM (49) and showed that this intermediate co-exists in three states (I, II and III) (Figure 7). The three states showed an assembled core and central protuberance. State 1 was the most similar to the *B. subtilis* 45S intermediate with densities for the L1 stalk and helices comprising the A, P and E sites (H89-93 and H68-71) not appearing in the cryo-EM map. However, unlike the 45S particle in *B. subtilis*, H97 and H42 in the L7/12 stalk were not latched (Figure 7, left panel). State II and III seemed to have passed the locked state and displayed density for the rRNA helices in the functional core. H97 and H42 in the L7/12 stalk were also latched in these two states

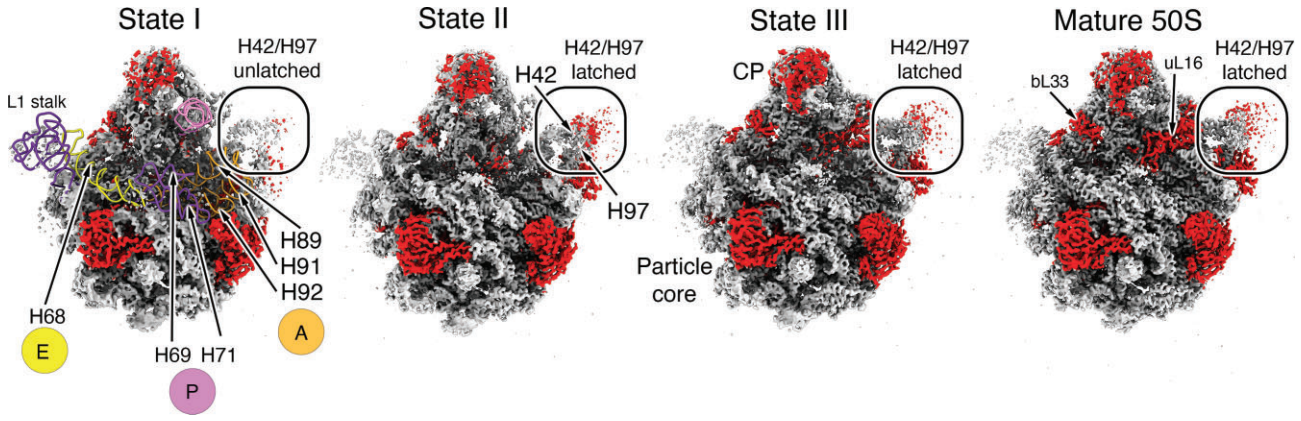

Figure 7. 50S assembly intermediates from an *E. coli* ΔrlmE strain. Cryo-EM structures of three 50S assembly intermediates purified from an *E. coli* strain lacking the rlmE gene. The panel in the right shows the cryo-EM structure of the mature 50S subunit purified from the same strain. The rRNA helices forming the A, P and E functional sites that are still not formed in state I are indicated. These helices adopt a mature conformation and show density in the cryo-EM maps for state II, III and 50S subunits. H42 and H97 forming the L7/L12 stalk are also indicated in each class. These two helices are unlatched in state I but latched in states 2 and 3 and the mature subunit. The rRNA in the cryo-EM maps is colored in light gray, and the r-proteins are shown in red. This figure was prepared from EMD entries 30 214 (state I), 30 213 (state II), 30 212 (state III) and 30 215 (mature 50S) (49).

(Figure 7, middle panels). The main difference between state II and III was the density of the r-protein uL16, which was absent in state II but present in state III.

These results suggest an important role of the U2552 methylation in licensing maturation of the functional sites in the 45S intermediate. However, the absence of RlmE does not fully prevent this step, as is the case of RbgA, YphC and YsxC in *B. subtilis*. In this case, maturation of the functional sites still proceeds. Therefore, it is likely that if a locking mechanism exists, additional factors are necessary. Three other factors, DbpA (50), ObgE (51) and EngA, also cause the accumulation of 45S-like particles when depleted from cells. Furthermore, the cold-sensitivity phenotype and accumulation of 45S particles in the Δ*rlmE* strain were alleviated by overexpression of *obgE* or *engA* (52). All these data suggest that in *E. coli*, the combined activities of these four factors implement the locking mechanisms in the 45S convergency. The details of this implementation are still unknown.

Interestingly, in the *B. subtilis* 45S particle H42 and H97 are critical for the locking mechanisms of this convergency intermediate. The binding of uL6 locks H42-H97 in a conformation that is released by RbgA, YphC and YsxC to continue the maturation process (Figure 3D). In *E. coli*, the intermediates with the closest structural similarity to the *B. subtilis* 45S intermediate, include the state I from the Δ*rlmE* strain (Figure 7, left panel), the E2 state in the iSAT reaction (Figure 5) (36), the E state in the genetic approach (41,43), and the C-CP-L28/L2 state in the 50S *in vitro* reconstitution study (Figure 4) (30). Conversely to the *B. subtilis* 45S particle, all these intermediates exhibit unlatched L7/12 stalk with H42 and H97 adopting a flexible conformation.

U2552 methylation promotes interdomain assembly between domains V (central protuberance) and IV (P and E functional site helices) and, promotes the incorporation of r-protein bL36 (47). The bL36 r-protein sits between helices H42 and H97, and its binding stabilizes these two helices (Figure 2B) and promotes the entry of uL16 and subsequent maturation of the central protuberance and the rRNA helices in the functional core. This is the process that states II and III from the Δ*rlmE* strain described (Figure 7, middle panels). Consequently, it seems the locking of the 45S particle in *E. coli* is implemented opposite to *B. subtilis*. When the 45S particle in *E. coli* is locked, the H42 and H97 helices adopt a flexible conformation. The action of RlmE and likely other factors (DbpA, ObgE and EngA) promotes stabilizing these two helices, releasing the lock and licensing progression of the 45S particle to the mature particle (53).

The existence of what seems to be an opposite locking mechanism of the 45S convergency point in *B. subtilis* and *E. coli* is consistent with the absence of a homolog of RlmE in *B. subtilus* and the fact that the U2552 in its 23S rRNA remains unmethylated. It is also consistent with the observation that RbgA is absent in *E. coli*, suggesting that these two opposite mechanisms do not coexist in one single species.

Altogether, existing literature suggests that convergency points in the 50S subunit assembly process may exist in multiple bacterial species. However, the locking mechanisms in these convergency assembly points differ between species. Mechanisms range from binding specific factors and r-proteins to the convergency intermediates, as observed in *B. subtilis*, to 23S rRNA modifications, as described for *E. coli*. Most likely, there are many other mechanisms still waiting to be discovered.

Do essential assembly factors acting at convergent assembly intermediates act independently, or in conjunction?

Recent cryo-EM structures of assembly intermediates from mitochondria in the human parasite *Trypanosoma brucei* showed that Mtg1, mt-EngA and mt-EngB, the mitochondrial homologues of RbgA, YphC and YsxC, bind simultaneously to the maturing large subunit along with 23 additional factors (Figure 8, left panel) (54,55). This finding strongly suggests that RbgA, YphC and YsxC in bacteria may also work coordinately to assist the assembly of the 50S subunit in bacteria. Given the structural and compositional similarities between the $45S_{RbgA}$, $45S_{YphC}$ and $44.5S_{YsxC}$ particles (Figure 2) that accumulate in the cell upon depletion of each one of these factors, it is possible that the assembling particles arrive at the convergency point represented by the 45S particle. The

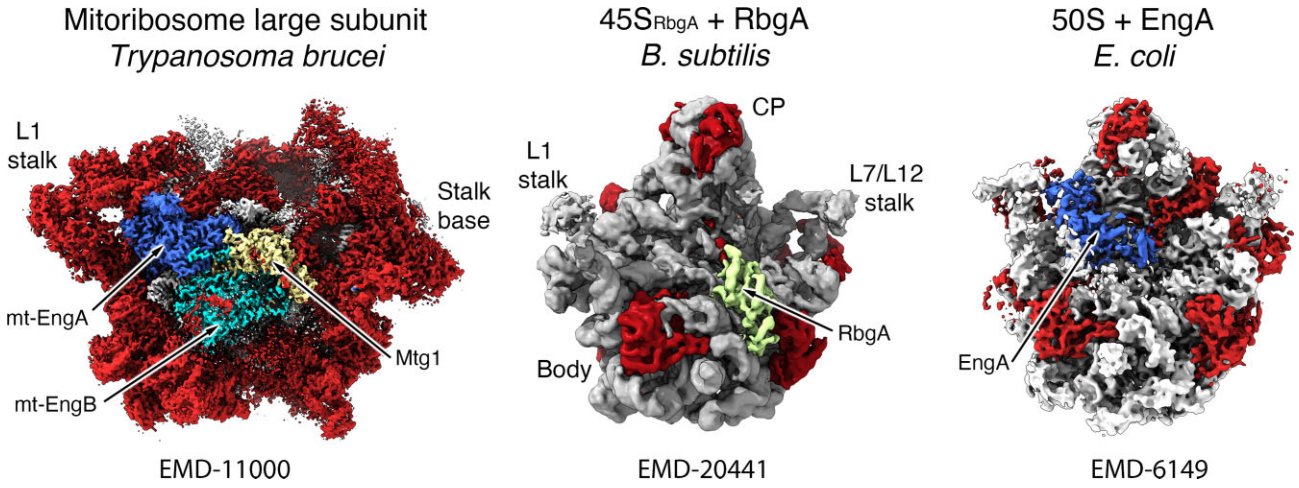

Figure 8. Assembly factors assisting convergent assembly intermediates in bacteria may act in conjuction. Left panel: Cryo-EM map of a mitoribosome large subunit assembly intermediate from *Trypanosome brucei* (EMD 11000) (left panel) (54) with assembly factors Mtg1 (RbgA homologue), mt-EngA (YphC homologue) and mt-EngB (YsxC homologue) bound simultaneously to the interface area of the subunit. Middle panel: Cryo-EM map of the *B. subtilis* 45S$_{RbgA}$ particle with RbgA, colored in yellow, bound to the P site (EMD 20441) (25). The binding site of RbgA in the subunit is equivalent to the binding site of Mtg1 in *T. Brucei*. Right panel: Cryo-EM map of the *E. coli* 50S subunit with EngA bound in the E site (EMD 6149) (60). The binding site of EngA (YphC homologue) in the subunit is equivalent to the binding site of mt-EngA in T. Brucei. There are no structures from protein homologues of mt-EngB bound to bacterial ribosomal subunits or assembly intermediates. In the three structures r-proteins are colored in red and rRNA is colored in light gray. Assembly factor mt-EngA and EngA are colored in dark blue and mt-EngB is colored in cyan.

three factors, RbgA, YphC and YsxC, may bind to the single intermediate and work in conjunction before the particle is licensed for further maturation steps, in which the A, P and E sites become functional. Whether binding of RbgA, YphC and YsxC occurs sequentially or simultaneously (as in the mitoribosomal particles) is still unknown. They may bind sequentially with each factor binding, performing its function independently and being released before the next factor binds. Alternatively, they may bind simultaneously and work together to catalyze the last maturation steps. According to binding assays, it has been discovered that RbgA, YphC, and YsxC are not very selective in their binding properties. Each of these factors can bind to any of 45S particles (45S$_{RbgA}$, 45S$_{YphC}$ and 44.5S$_{YsxC}$). Additionally, it is also possible for more than one of these factors to bind simultaneously to the particles (16). However, further structural analyses are required to elucidate if they exert their functions simultaneously or sequentially. This is an important aspect to be resolved, given that the precise mechanisms of action of these factors at this convergent intermediate will determine whether the maturation of the A, P and E sites follows a precise sequence.

Conclusions and remaining questions

Using powerful image classification tools, recent cryo-EM studies allowed us to visualize dozens of ribosome assembly intermediates in multiple bacterial species. As a result, a more defined picture of the ribosome assembly process is emerging. A relevant question is whether critical steps exist in the ribosomal assembly process. In *B. subtilis*, one of these critical steps was recently identified and characterized (17). This step represents a merging point where all parallel assembly pathways of the 50S ribosomal subunit converge. Whether the assembly process of the 50S subunit exhibits convergency points in other bacterial species is still unclear. In other model bacteria such as *E. coli*, cryo-EM has identified a locked convergency point, but in those cases, the locking mechanism seems to be different from *B. subtilis* and how factors regulate this maturation step still needs to be fully revealed. For other bacterial species, experiments similar to those done in *B. subtilis* and *E. coli* have not yet been done. These studies are essential to figuring out whether convergency points in the maturation process of the 50S subunit are a common theme among bacteria and how their locking and unlocking mechanisms are implemented. It will also be important to elucidate whether convergency points are present in the assembly pathways for the small 30S subunits. Finally, a fascinating avenue will be to perform targeted experiments to analyze the existence of these intermediates in the assembly process of the cytosolic and mitochondrial ribosomes in eukaryotes.

Data availability

No new data were generated or analysed in support of this research.

Acknowledgements

We thank members of the Ortega Lab for their always helpful discussions and many of the findings describe in this review.

Funding

Canadian Institutes of Health Research [PJT-153044 to J.O.]; DFG (German Research Foundation) [SPP2191, 506373047 to R.N.]. Funding for open access charge: Canadian Institutes of Health Research.

Conflict of interest statement

The authors declare no competing financial interests. The funders had no role in study design, data collection and analysis, decision to publish, or manuscript preparation.

References

1. Gutgsell,N.S. and Jain,C. (2012) Gateway role for rRNA precursors in ribosome assembly. *J. Bacteriol.*, **194**, 6875–6882.
2. Traub,P. and Nomura,M. (1969) Studies on the assembly of ribosomes in vitro. *Cold Spring Harb. Symp. Quant. Biol.*, **34**, 63–67.
3. Rohl,R. and Nierhaus,K.H. (1982) Assembly map of the large subunit (50S) of Escherichia coli ribosomes. *Proc. Natl. Acad. Sci. U.S.A.*, **79**, 729–733.
4. Woodson,S.A. (2008) RNA folding and ribosome assembly. *Curr. Opin. Chem. Biol.*, **12**, 667–673.
5. Woodson,S.A. (2011) RNA folding pathways and the self-assembly of ribosomes. *Acc. Chem. Res.*, **44**, 1312–1319.
6. Adilakshmi,T., Bellur,D.L. and Woodson,S.A. (2008) Concurrent nucleation of 16S folding and induced fit in 30S ribosome assembly. *Nature*, **455**, 1268–1272.
7. Duss,O., Stepanyuk,G.A., Grot,A., O'Leary,S.E., Puglisi,J.D. and Williamson,J.R. (2018) Real-time assembly of ribonucleoprotein complexes on nascent RNA transcripts. *Nat. Commun.*, **9**, 5087.
8. Duss,O., Stepanyuk,G.A., Puglisi,J.D. and Williamson,J.R. (2019) Transient protein-RNA interactions guide nascent ribosomal RNA folding. *Cell*, **179**, 1357–1369.
9. Rodgers,M.L. and Woodson,S.A. (2019) Transcription increases the cooperativity of Ribonucleoprotein assembly. *Cell*, **179**, 1370–1381.
10. Shajani,Z., Sykes,M.T. and Williamson,J.R. (2011) Assembly of bacterial ribosomes. *Annu. Rev. Biochem.*, **80**, 501–526.
11. Sergeeva,O.V., Bogdanov,A.A. and Sergiev,P.V. (2015) What do we know about ribosomal RNA methylation in Escherichia coli?*Biochimie*, **117**, 110–118.
12. Ofengand,J. (2002) Ribosomal RNA pseudouridines and pseudouridine synthases. *FEBS Lett.*, **514**, 17–25.
13. Talkington,M.W., Siuzdak,G. and Williamson,J.R. (2005) An assembly landscape for the 30S ribosomal subunit. *Nature*, **438**, 628–632.
14. Kim,H., Abeysirigunawarden,S.C., Chen,K., Mayerle,M., Ragunathan,K., Luthey-Schulten,Z., Ha,T. and Woodson,S.A. (2014) Protein-guided RNA dynamics during early ribosome assembly. *Nature*, **506**, 334–338.
15. Jomaa,A., Jain,N., Davis,J.H., Williamson,J.R., Britton,R.A. and Ortega,J. (2014) Functional domains of the 50S subunit mature late in the assembly process. *Nucleic Acids Res.*, **42**, 3419–3435.
16. Ni,X., Davis,J.H., Jain,N., Razi,A., Benlekbir,S., McArthur,A.G., Rubinstein,J.L., Britton,R.A., Williamson,J.R. and Ortega,J. (2016) YphC and YsxC GTPases assist the maturation of the central protuberance, GTPase associated region and functional core of the 50S ribosomal subunit. *Nucleic Acids Res.*, **44**, 8442–8455.
17. Seffouh,A., Trahan,C., Wasi,T., Jain,N., Basu,K., Britton,R.A., Oeffinger,M. and Ortega,J. (2022) RbgA ensures the correct timing in the maturation of the 50S subunits functional sites. *Nucleic Acids Res.*, **50**, 10801–10816.
18. Chen,S.S., Sperling,E., Silverman,J.M., Davis,J.H. and Williamson,J.R. (2012) Measuring the dynamics of E. coli ribosome biogenesis using pulse-labeling and quantitative mass spectrometry. *Mol. Biosyst.*, **8**, 3325–3334.
19. Lindahl,L. (1975) Intermediates and time kinetics of the in vivo assembly of Escherichia coli ribosomes. *J. Mol. Biol.*, **92**, 15–37.
20. Nikolay,R., Hilal,T., Qin,B., Mielke,T., Burger,J., Loerke,J., Textoris-Taube,K., Nierhaus,K.H. and Spahn,C.M.T. (2018) Structural visualization of the formation and activation of the 50S ribosomal subunit during In vitro reconstitution. *Mol. Cell*, **70**, 881–893.
21. Davis,J.H. and Williamson,J.R. (2017) Structure and dynamics of bacterial ribosome biogenesis. *Philos. Trans. Roy. Soc. Lond. Ser. B Biol. Sci.*, **372**, 20160181.
22. Guo,Q., Goto,S., Chen,Y., Feng,B., Xu,Y., Muto,A., Himeno,H., Deng,H., Lei,J. and Gao,N. (2013) Dissecting the in vivo assembly of the 30S ribosomal subunit reveals the role of RimM and general features of the assembly process. *Nucleic Acids Res.*, **41**, 2609–2620.
23. Jomaa,A., Stewart,G., Martin-Benito,J., Zielke,R., Campbell,T.L., Maddock,J.R., Brown,E.D. and Ortega,J. (2011) Understanding ribosome assembly: the structure of in vivo assembled immature 30S subunits revealed by cryo-electron microscopy. *RNA*, **17**, 697–709.
24. Razi,A., Davis,J.H., Hao,Y., Jahagirdar,D., Thurlow,B., Basu,K., Jain,N., Gomez-Blanco,J., Britton,R.A., Vargas,J., *et al.* (2019) Role of era in assembly and homeostasis of the ribosomal small subunit. *Nucleic Acids Res.*, **47**, 8301–8317.
25. Seffouh,A., Jain,N., Jahagirdar,D., Basu,K., Razi,A., Ni,X., Guarne,A., Britton,R.A. and Ortega,J. (2019) Structural consequences of the interaction of RbgA with a 50S ribosomal subunit assembly intermediate. *Nucleic Acids Res.*, **47**, 10414–10425.
26. Sun,J., Kinman,L., Jahagirdar,D., Ortega,J. and Davis,A.J. (2022) KsgA facilitates ribosomal small subunit maturation by proofreading a key structural lesion. *Biorxiv*, **30**, 1468–1480.
27. Leong,V., Kent,M., Jomaa,A. and Ortega,J. (2013) Escherichia coli rimM and yjeQ null strains accumulate immature 30S subunits of similar structure and protein complement. *RNA*, **19**, 789–802.
28. Dohme,F. and Nierhaus,K.H. (1976) Total reconstitution and assembly of 50 S subunits from Escherichia coli ribosomes in vitro. *J. Mol. Biol.*, **107**, 585–599.
29. Nierhaus,K.H. (1991) The assembly of prokaryotic ribosomes. *Biochimie*, **73**, 739–755.
30. Qin,B., Lauer,S.M., Balke,A., Vieira-Vieira,C.H., Burger,J., Mielke,T., Selbach,M., Scheerer,P., Spahn,C.M.T. and Nikolay,R. (2023) Cryo-EM captures early ribosome assembly in action. *Nat. Commun.*, **14**, 898.
31. Jewett,M.C., Fritz,B.R., Timmerman,L.E. and Church,G.M. (2013) In vitro integration of ribosomal RNA synthesis, ribosome assembly, and translation. *Mol. Syst. Biol.*, **9**, 678.
32. Fritz,B.R. and Jewett,M.C. (2014) The impact of transcriptional tuning on in vitro integrated rRNA transcription and ribosome construction. *Nucleic Acids Res.*, **42**, 6774–6785.
33. Hammerling,M.J., Fritz,B.R., Yoesep,D.J., Kim,D.S., Carlson,E.D. and Jewett,M.C. (2020) In vitro ribosome synthesis and evolution through ribosome display. *Nat. Commun.*, **11**, 1108.
34. Liu,Y., Davis,R.G., Thomas,P.M., Kelleher,N.L. and Jewett,M.C. (2021) In vitro-constructed ribosomes enable multi-site incorporation of noncanonical amino acids into proteins. *Biochemistry*, **60**, 161–169.
35. Groisman,E.A. and Chan,C. (2021) Cellular adaptations to cytoplasmic Mg(2+) limitation. *Annu. Rev. Microbiol.*, **75**, 649–672.
36. Dong,X., Doerfel,L.K., Sheng,K., Rabuck-Gibbons,J.N., Popova,A.M., Lyumkis,D. and Williamson,J.R. (2023) Near-physiological in vitro assembly of 50S ribosomes involves parallel pathways. *Nucleic Acids Res.*, **51**, 2862–2876.
37. Uicker,W.C., Schaefer,L. and Britton,R.A. (2006) The essential GTPase RbgA (YlqF) is required for 50S ribosome assembly in Bacillus subtilis. *Mol. Microbiol.*, **59**, 528–540.
38. Schaefer,L., Uicker,W.C., Wicker-Planquart,C., Foucher,A.E., Jault,J.M. and Britton,R.A. (2006) Multiple GTPases participate in the assembly of the large ribosomal subunit in Bacillus subtilis. *J. Bacteriol.*, **188**, 8252–8258.
39. Gulati,M., Jain,N., Davis,J.H., Williamson,J.R. and Britton,R.A. (2014) Functional interaction between ribosomal protein L6 and RbgA during ribosome assembly. *PLos Genet.*, **10**, e1004694.
40. Roy-Chaudhuri,B., Kirthi,N. and Culver,G.M. (2010) Appropriate maturation and folding of 16S rRNA during 30S subunit biogenesis are critical for translational fidelity. *Proc. Natl. Acad. Sci. U.S.A.*, **107**, 4567–4572.
41. Davis,J.H., Tan,Y.Z., Carragher,B., Potter,C.S., Lyumkis,D. and Williamson,J.R. (2016) Modular assembly of the bacterial large ribosomal subunit. *Cell*, **167**, 1610–1622.

42. Rabuck-Gibbons,J.N., Popova,A.M., Greene,E.M., Cervantes,C.F., Lyumkis,D. and Williamson,J.R. (2020) SrmB rescues trapped ribosome assembly intermediates. *J. Mol. Biol.*, **432**, 978–990.
43. Rabuck-Gibbons,J.N., Lyumkis,D. and Williamson,J.R. (2022) Quantitative mining of compositional heterogeneity in cryo-EM datasets of ribosome assembly intermediates. *Structure*, **30**, 498–509.
44. Sheng,K., Li,N., Rabuck-Gibbons,J.N., Dong,X., Lyumkis,D. and Williamson,J.R. (2023) Assembly landscape for the bacterial large ribosomal subunit. *Nat. Commun.*, **14**, 5220.
45. Li,N., Chen,Y., Guo,Q., Zhang,Y., Yuan,Y., Ma,C., Deng,H., Lei,J. and Gao,N. (2013) Cryo-EM structures of the late-stage assembly intermediates of the bacterial 50S ribosomal subunit. *Nucleic Acids Res.*, **41**, 7073–7083.
46. Sieber,G. and Nierhaus,K.H. (1978) Kinetic and thermodynamic parameters of the assembly in vitro of the large subunit from Escherichia coli ribosomes. *Biochemistry*, **17**, 3505–3511.
47. Arai,T., Ishiguro,K., Kimura,S., Sakaguchi,Y., Suzuki,T. and Suzuki,T. (2015) Single methylation of 23S rRNA triggers late steps of 50S ribosomal subunit assembly. *Proc. Natl. Acad. Sci. U.S.A.*, **112**, E4707–E4716.
48. Ishiguro,K., Arai,T. and Suzuki,T. (2019) Depletion of S-adenosylmethionine impacts on ribosome biogenesis through hypomodification of a single rRNA methylation. *Nucleic Acids Res.*, **47**, 4226–4239.
49. Wang,W., Li,W., Ge,X., Yan,K., Mandava,C.S., Sanyal,S. and Gao,N. (2020) Loss of a single methylation in 23S rRNA delays 50S assembly at multiple late stages and impairs translation initiation and elongation. *Proc. Natl. Acad. Sci. U.S.A.*, **117**, 15609–15619.
50. Sharpe Elles,L.M., Sykes,M.T., Williamson,J.R. and Uhlenbeck,O.C. (2009) A dominant negative mutant of the E. coli RNA helicase DbpA blocks assembly of the 50S ribosomal subunit. *Nucleic Acids Res.*, **37**, 6503–6514.
51. Jiang,M., Datta,K., Walker,A., Strahler,J., Bagamasbad,P., Andrews,P.C. and Maddock,J.R. (2006) The Escherichia coli GTPase CgtAE is involved in late steps of large ribosome assembly. *J. Bacteriol.*, **188**, 6757–6770.
52. Tan,J., Jakob,U. and Bardwell,J.C. (2002) Overexpression of two different GTPases rescues a null mutation in a heat-induced rRNA methyltransferase. *J. Bacteriol.*, **184**, 2692–2698.
53. Nikolay,R., Hilal,T., Schmidt,S., Qin,B., Schwefel,D., Vieira-Vieira,C.H., Mielke,T., Burger,J., Loerke,J., Amikura,K., *et al.* (2021) Snapshots of native pre-50S ribosomes reveal a biogenesis factor network and evolutionary specialization. *Mol. Cell*, **81**, 1200–1215.
54. Jaskolowski,M., Ramrath,D.J.F., Bieri,P., Niemann,M., Mattei,S., Calderaro,S., Leibundgut,M., Horn,E.K., Boehringer,D., Schneider,A., *et al.* (2020) Structural insights into the mechanism of mitoribosomal large subunit biogenesis. *Mol. Cell*, **79**, 629–644.
55. Tobiasson,V., Gahura,O., Aibara,S., Baradaran,R., Zikova,A. and Amunts,A. (2021) Interconnected assembly factors regulate the biogenesis of mitoribosomal large subunit. *EMBO J.*, **40**, e106292.
56. Sohmen,D., Chiba,S., Shimokawa-Chiba,N., Innis,C.A., Berninghausen,O., Beckmann,R., Ito,K. and Wilson,D.N. (2015) Structure of the Bacillus subtilis 70S ribosome reveals the basis for species-specific stalling. *Nat. Commun.*, **6**, 6941.
57. Palacios,A. (2022) Direct visualization of the roles of the essential GTPases YphC and YsxC in the assembly of the bacterial ribosome. Master Thesis.
58. Herold,M. and Nierhaus,K.H. (1987) Incorporation of six additional proteins to complete the assembly map of the 50 S subunit from Escherichia coli ribosomes. *J. Biol. Chem.*, **262**, 8826–8833.
59. Chen,S.S. and Williamson,J.R. (2013) Characterization of the ribosome biogenesis landscape in E. coli using quantitative mass spectrometry. *J. Mol. Biol.*, **425**, 767–779.
60. Zhang,X., Yan,K., Zhang,Y., Li,N., Ma,C., Li,Z., Zhang,Y., Feng,B., Liu,J., Sun,Y., *et al.* (2014) Structural insights into the function of a unique tandem GTPase EngA in bacterial ribosome assembly. *Nucleic Acids Res.*, **42**, 13430–13439.

Received: September 14, 2023. **Revised:** March 2, 2024. **Editorial Decision:** March 6, 2024. **Accepted:** March 7, 2024